Implementation of Controller Design for an Unmanned Aerial Vehicle Helicopter

Chaw Ei San*, Hla Myo Tun*, Zaw Min Naing**

* Department of Electronic Engineering, Mandalay Technological University
** Technological University (Maubin)

Abstract- The overall objective with this paper is to evaluate a method for designing nonlinear controllers in aircrafts with concern in robustness against modeling insecurities and also to minimize the design effort. The later objective is of great importance since there exists, in the industry, an ambition to automatize the design for as far extend as possible. The nonlinear method, State Dependent Riccati Equation (SDRE), used in this work is a nonlinear version of classic LQ design and both are evaluated and compared for a few flying conditions. Also another nonlinear control method is tested. LQ and SDRE show equal performance during both looping and more complicated maneuvers, such as high angle of attack wind-vector roll. Further it is possible to automatize the LQ design as well as it is possible for SDRE. Still SDRE is preferable since it will always be somewhat more accurate than LQ. A Monte Carlo simulation is made on LQ and SDRE showing that the model is robust against relatively large modeling error of 40%.

Index Terms- URAV, MATLAB, SIMULINK, Stability Analysis, Surveillance System

I. Introduction

IN cmodern aircraft design it is vital to quickly be able to develop a controller that will give dynamics which are reasonably close to the desired dynamics in order to gain sufficient understanding of various aspects of the proposed aircraft concept. The main focus is normally on maneuver- and control properties, including handling qualities and actuator effectiveness, properties which are commonly appraised via simulations. To be able to design a controller at an early stage in an aircraft design is especially important in the design of modern fighters and unmanned aerial vehicles (UAVs) since such aircraft can be aerodynamically unstable, at certain speeds, in both pitch and yaw. This means that even basic maneuvering properties cannot be evaluated without the existence of a stabilizing controller. Aircraft dynamics are most often described (without concern of aero elastic effects) by Newton-Euler's nonlinear rigid body equations, formulated in a vehicle fixed coordinate system. The forces and moments that act on the body, and which can be altered by the control surfaces, are nonlinear functions of the states in the equations of motion. This makes it natural to use nonlinear control theory in the design of controllers. Key aspects of concern are then stability, robustness and performance. In the present work we concentrate on these aspects for the State Dependent Riccati Equation (SDRE) nonlinear design method applied to a realistic model of an UAV is illustrated in Fig.1.

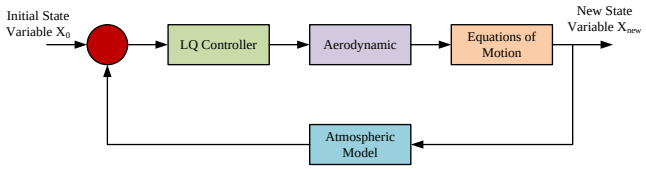

Fig.1. Proposed Block Diagram of UAV System.

II. Aircraft Dynamics

In modern aircraft design it is vital to quickly be able to develop a controller that will give dynamics which are reasonably close to the desired dynamics in order to gain sufficient understanding of various aspects of the proposed aircraft concept. The main focus is normally on maneuver- and control properties, including handling qualities and actuator effectiveness, properties which are commonly appraised via simulations. To be able to design a controller at an early stage in an aircraft design is especially important in the design of modern fighters and unmanned aerial vehicles (UAVs) since such aircraft can be aerodynamically unstable, at certain speeds, in both pitch and yaw. This means that even basic maneuvering properties cannot be evaluated without the existence of a stabilizing controller.

Aircraft dynamics are most often described (without concern of aero elastic effects) by Newton-Euler's nonlinear rigid body equations, formulated in a vehicle fixed coordinate system. The forces and moments that act on the body, and which can be altered by the control surfaces, are nonlinear functions of the states in the equations of motion. This makes it natural to use nonlinear control theory in the design of controllers. Key aspects of concern are then stability, robustness and performance.

The Newton-Euler equations of motion for a rigid body are given by the equations for the rate of change of the linear and angular momentum, p and ℓ, respectively, commonly formulated around the center of mass (CoM) in an inertial coordinate system as

$$\dot{p} = f, \quad (1)$$

$$\dot{\ell} = m, \quad (2)$$

where f and m denote the total external force and total external moment around CoM, respectively. If both sides of (2.1), (2.2) are expressed in terms of a Cartesian body-fixed coordinate system centered in CoM, they can be rewritten on the familiar form [3]

$$F = \dot{m}V + m\dot{V} + \omega \times mV, \quad (3)$$

$$M = \dot{I}\omega + I\dot{\omega} + \omega \times I\omega, \quad (4)$$

where V =[u, v,w]
T and ω =[p, q, r]

T are the velocity and angular velocity, respectively, F and M are the force and moment, respectively, and m and I are the mass and inertia matrix, respectively (all in body coordinates). If we assume that m and I both are constant then the Equation (3) and (4) reduce to

$$m\dot{V} = -\omega \times mV + F, \quad (5)$$

$$I\dot{\omega} = -\omega \times I\omega + M, \quad (6)$$

which is the most often used form of the force and moment equations in flight mechanics. In our applications the sum F of external body forces is divided into gravitational and other external forces (aerodynamically and thrust) as $F = F_g + Fe$. The equations in (5) and (6) will be the basis for our modeling of the motion of the aircraft.

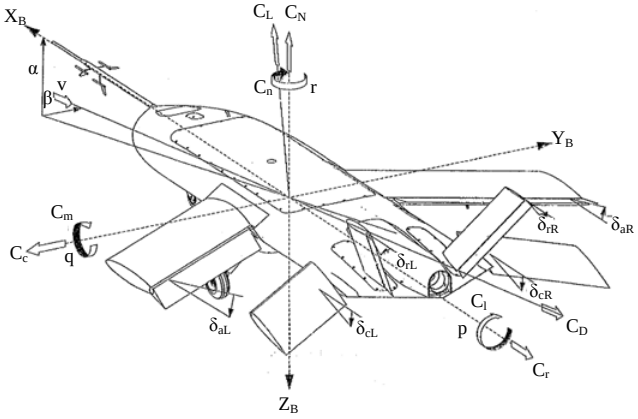

Fig.2. Definitions of the coordinate system and the aerodynamic angles

The aircraft is symmetric in the x, z-plane and the inertia cross products Ixy and Iyz are therefore zero. Further, Ixz is small in comparison with Ixx, Iyy and Izz and is therefore neglected. The matrix of inertia is therefore of the diagonal form

$$I=\begin{bmatrix} I_{xx} & 0 & 0 \\ 0 & I_{yy} & 0 \\ 0 & 0 & I_{zz} \end{bmatrix} \quad (7)$$

The aerodynamic angles α, angle of attack, and β, sideslip angle, are defined in terms of the x, y and z-components of the velocity V as

$$u = V\cos\alpha\cos\beta,$$
$$v = V\sin\beta,$$
$$w = V\sin\alpha\cos\beta, \quad (8)$$

where $V = \sqrt{[u2 + v2 + w2]}$ is the absolute velocity. In Fig.2 the standard vehicle Cartesian coordinate system and the definitions of α and β are illustrated. The vector Fg of gravitational body forces is given by

$$F_g = [-g\sin\theta, g\cos\theta\sin\varphi, g\cos\theta\cos\varphi]^T, \quad (9)$$

where g is the gravitational acceleration constant and φ, θ are the Euler bank angle and pitch angle, respectively. If the vector Fe of other external forces (apart from gravity) are expressed as Fe =[X, Y,Z] ^{T} and the vector of external moments M as M =[L,M,N] ^{T} the force and moment equations (5) and (6) can be written in component form as

$$\dot{u} = vr - wq - g\sin\theta + X/m,$$
$$\dot{v} = wp - ur + g\cos\theta\sin\varphi + Y/m,$$
$$\dot{w} = uq - vp + g\cos\theta\cos\varphi + Z/m,$$
$$\dot{p} = qr(Iyy - Izz)/Ixx + L/Ixx,$$
$$\dot{q} = rp(Izz - Ixx)/Iyy + M/Iyy,$$
$$\dot{r} = pq(Ixx - Iyy)/Izz + N/Izz. \quad (10)$$

These six equations represent the standard six-degree of freedom (6DOF) model for aircraft dynamics used in the literature [3]. To complete the dynamical model of the aircraft, the dynamical relations also for the Euler angles and the inertial position are needed. The dynamical equations for the Euler angles φ, θ and ψ are given in terms of the body velocities and angular velocities as

$$\dot{\varphi} = p + q\sin\varphi\tan\theta + r\cos\varphi\tan\theta,$$
$$\dot{\theta} = q\cos\varphi - r\sin\varphi,$$
$$\dot{\psi} = q\sin\theta\sec\varphi + r\cos\varphi\sec\theta, \quad (11)$$

and the relations for the inertial position coordinates x_e, y_e and z_e are

$$\dot{x}_e = u\cos\theta\cos\psi + v(\sin\varphi\sin\theta\cos\psi - \cos\varphi\cos\psi) + w(\cos\varphi\sin\theta\cos\psi + \sin\varphi\sin\psi),$$
$$\dot{y}_e = u\cos\theta\sin\psi + v(\sin\varphi\sin\theta\sin\psi + \cos\varphi\cos\psi) + w(\cos\varphi\sin\theta\sin\psi + \sin\varphi\cos\psi),$$
$$\dot{z}_e = -u\sin\theta + v\sin\varphi\cos\theta + w\cos\varphi\cos\theta. \quad (12)$$

The derivatives of the Euler angles are found from geometric relations and the last three equations are a coordinate transformation from body coordinates frame to the earth coordinates [3]. The aerodynamical forces are most conveniently expressed in terms of the aerodynamical angles α, β and therefore it is convenient to represent the first three equations in (10) in terms of α, β. By solving for α, β in (.9), taking the time derivative and using (10) it can be obtained

$$\dot{\alpha} = \frac{\cos(\alpha)}{V\cos(\beta)}\left(\frac{Z}{m}\right) - p\cos(\alpha)\tan(\beta) + q - r\sin(\alpha)\tan(\beta) - \frac{\sin(\alpha)}{V\cos(\beta)}\left(\frac{X}{m}\right),$$

$$\dot{\beta} = \frac{\cos(\beta)}{V}\left(\frac{Y}{m}\right) + p\sin(\alpha) - r\cos(\alpha) - \frac{\cos(\alpha)\sin(\beta)}{V}\left(\frac{X}{m}\right) - \frac{\sin(\alpha)\sin(\beta)}{V}\left(\frac{Z}{m}\right) \quad (13)$$

Since the absolute velocity often varies on a somewhat slower timescale compared to the other variables, it is common to make the simplifying assumption that

$$\dot{V} = 0, \quad (14)$$

which also shall be done here. This completes our basic dynamical description of the aircraft motion.

Modeling the URAV Aerodynamics using MATLAB

With the data above and by the help of using MATLAB, the A & B matrices were constructed. In order to make a quick check for the output response using MATLAB, the following commands are executed to test the effect of applying 1 degree of collecting pitching for 5 seconds:

```
t=0:0.01:5;
de=1*pi/180*ones(size(t));
[n1,d]=ss2tf(A,B,C,D,1);
sys = tf(n1(2,:),d);
lsim(sys,de,t);
```

The simulation shows a linear and continuous vertical acceleration to about 10m/s after 5 seconds. The simulation shows clearly that the system is unstable and it produces diverging response.

The positive real parts of the eigenvalues which indicates the system is unstable. The system needs a state feedback matrix K to ensure that the system is stable. The matrix K will be obtained using the method of linear-quadratic (LQ) state-feedback regulator for continuous plant.

$$\dot{X}=[A-BK]x+Bu$$
$$Y=Qx$$

This can be easily solved for using the function (LQR) in MATLAB. The Q matrix is chosen to be an identity matrix of 8-by-8 in dimension:

```
C = diag(ones(1,8));
[K]= lqr (A,B,C,diag([1 1 1 1]));
```

Now all the real parts of the eigenvalues are negative which indicate a stable system. To obtain the transfer function using MATLAB, the following commands were executed:

```
[K]= lqr (A,B,Q,diag([1 1 1 1]))
p=85;
[n1,d]=ss2tf(A-B*K,B,p*C,D,1);
[n2,d]=ss2tf(A-B*K,B,p*C,D,2);
[n3,d]=ss2tf(A-B*K,B,p*C,D,3);
[n4,d]=ss2tf(A-B*K,B,p*C,D,4);
tf(n1(2,:),d)
step(5*pi/180*n1(2,:),d)
```

The weighting factor (p) has been selected to be 85 after little iteration to produce the maximum vertical speed at a reasonable collective pitch angle. The above commands will results of having 8 numerator equations for each of the 4 tf(n1(2,:),d) will output the flight transfer inputs.

III. Transfer Function Evaluation

Non-dimensional stability and control derivatives estimated are shown in the following, and dimensional stability and control derivatives are calculated by the following equations.

Lift coefficient, C_L 0.2866

Drag coefficient, C_D 0.0358

Drag coefficient at zero lift, C_{D_o} 0.0311

Lift curve slope of the horizontal tail, C_{L_α} 4.1417

Variation of drag coefficient with angle of attack, C_{D_α} 0.1370

Variation of pitching moment coefficient with angle of attack, C_{m_α} -1.0636

Variation of lift coefficient with rate of change angle of attack, $C_{L_{\dot{\alpha}}}$ 1.5787

Variation of pitching moment coefficient with rate of change angle of attack, $C_{m_{\dot{\alpha}}}$ -4.6790

Variation of lift coefficient with pitch rate, C_{L_q} 3.9173

Variation of pitching moment coefficient with pitch rate, C_{m_q} -11.6918

Variation of lift coefficient with elevator deflection, $C_{L_{\delta e}}$ 0.4130

Variation of pitching moment coefficient with elevator deflection, $C_{m_{\delta e}}$ -1.2242

Variation of drag coefficient with elevator deflection, $C_{D_{\delta e}}$ 0.0650

Sea level air density, ρ $= 0.002378$ (slug.ft^{-3})

Gravitational constant, g $= 32.174$ (lb.ft^{-2})

Weight, w $= m \times g$ (15)

Mass or pitching moment, $m = \frac{w}{g}$

$$= \frac{57.79\,\text{lb}}{32.174\,\text{lb.ft}^{-2}}$$

$= 1.7962$ (slugs)

Dynamic pressure, Q $= \frac{1}{2}\rho u_o^2$ (16)

$= (0.5)\,(0.002378$ slug ft$^{-3})\,(88$ ft.s$^{-1})$

$= 9.2076$ (lb.ft^{-2})

QS $= (9.2076$ lb.ft$^{-2})\,(22.38$ ft$^2)$

$= 206.0661$ (lb)

$QS\,\bar{c}$ $= (206.0661$ lb$)\,(5.7$ ft$)$

$= 1174.5768$ (ft.lb)

$\bar{c}/2u_0$ $= (5.7$ ft$) / (2 \times 88$ ft.s$^{-1})$

$= 0.0324$ (s)

For u derivatives,

$X_u = -(C_{D_u} + 2C_{D_o})\,QS / (u_0 m)$ (17)

$= -[0.0 + 2(0.0311)]\,(206.0661$ lb$) / [(88$ ft.s$^{-1})\,(1.7962$ slugs$)] = -0.0933$ (s^{-1})

$Z_u = -\left(C_{L_u} + 2C_{L_0}\right) QS / (u_0 m)$ (18)

$= -[0.0 + 2(0.2866)]\ (206.0661\ lb) / [(88\ ft.s^{-1})\ (1.7962\ slugs)] = -0.7473\ (s^{-1})$

$M_u = 0$

For w derivatives,

$X_w = -\left(C_{D_\alpha} - C_{L_0}\right) QS / (u_0 m)$ (19)

$= -(0.1370 - 0.2866)\ (206.0661\ lb) / [(88\ ft.s^{-1})\ (1.7962\ slugs)]$

$= 0.1950\ (s^{-1})$

$Z_w = -\left(C_{L_\alpha} + C_{D_o}\right) QS / (u_0 m)$ (20)

$= -(4.1417 + 0.0311)\ (206.0661\ lb) / [(88\ ft.s^{-1})\ (1.7962\ slugs)]$

$= -5.44\ (s^{-1})$

$M_w = C_{m_\alpha} QS\bar{c} / (u_0 I_y)$ (21)

$= (-1.0636)\ (1174.5768\ ft.lb) / [(88\ ft.s^{-1})\ (13.21\ slug.ft^2)]$

$= -1.0747\ [1 / (ft.s)]$

For $\dot{w}$ derivatives,

$X_{\dot{w}} = 0$

$Z_{\dot{w}} = 0$

$M_{\dot{w}} = C_{m_{\dot{\alpha}}} \frac{\bar{c}}{2u_0} QS\bar{c} / (u_0 I_y)$ (22)

$= (-4.6790)\ (0.0324\ s)\ (1174.5768\ ft.lb) / [\ (88\ ft.s^{-1})\ (13.21\ slug.ft^2)]$

$= -0.1531(ft^{-1})$

For q derivatives,

$X_q = 0$

$Z_q = 0$

$M_q = C_{m_q} \frac{\bar{c}}{2u_0} QS\bar{c} / I_y$ (23)

$= (-11.6918)\ (0.0324\ s)\ (1174.5768\ ft.lb) / (13.21\ slug.ft^2)$

$= -33.6684\ (s^{-1})$

For δe derivatives,

$X_{\delta e} = C_{D_{\delta e}} \times QS/m$ (24)

$= 0.0650$ x $(206.0661\ lb) / (1.7962\ slugs)$

$= 7.4570\ (ft / s^2)$

$Z_{\delta e} = C_{L_{\delta e}} \times QS/m$ (25)

$= 0.4130$ x $(206.0661\ lb) / (1.7962\ slugs)$

$= 47.3807\ (ft / s^2)$

$M_{\delta e} = C_{m_{\delta e}} \times QS\bar{c} / I_y$ (26)

$= (-1.2242)\ (1174.5768\ ft.lb) / (13.21\ slug.ft^2)$

$= -108.8506\ (s^{-2})$

IV. System Flowchart

The procedure will start from the translational and rotational dynamics and rotational equations of motion. There are certain assumptions made for the sake of simplifications. Based on the stability control system, the implementation of mathematical model and test for observer control system is developed. Fig.3 is the flowchart for conceptual design process.

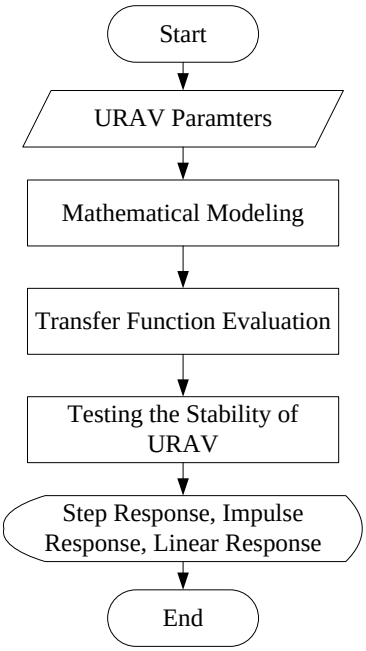

Fig.3. System Flowchart

V. Controller Design Using SIMULINK

The observer controller design takes into consideration that not all states can be sensed and there for the addition of an observer is needed in the system. This addition requires an additional loop in the controller and a second loop gain, the observer gain, L. The observer gain design is theoretically independent of the controller feedback gain design (K). However, in this case the gain, L, was calculated by pole placement based on the closed loop poles of the controller system with the gain K. The best system performance was achieved by placing the observer gain poles to be equal to the negative of the smallest magnitude of the real component of the closed loop controller poles.

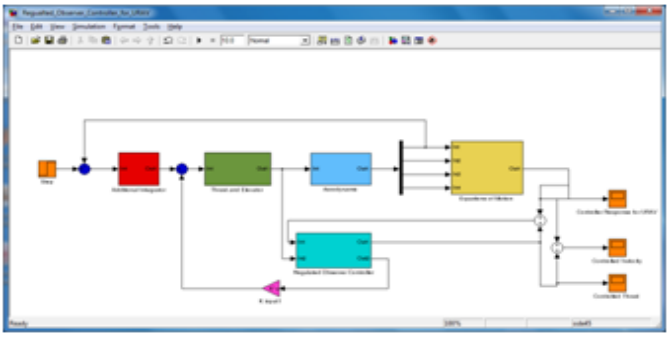

Fig.4. SIMULINK Model for URAV with Controller Design

VI. Simulation Results for Regulated Observer Controller

Based on the theoretical background on the Global Hawk URAV, the SIMULINK model is to analyze the observer controller design. The simulation results are developed according to the thrust and velocity condition of Global Hawk URAV. The thrust saturation and elevator saturation are supported to investigate the observer controller response of Global Hawk URAV.

The regulated controller response for Global Hawk URAV is mentioned in Fig.5. The sample time for thrust and velocity noise are set to 0.02 for good situation. The yellow color response is the velocity response with its noise. According to this response, the Global Hawk URAV is met with the high performance situation for stability analysis.

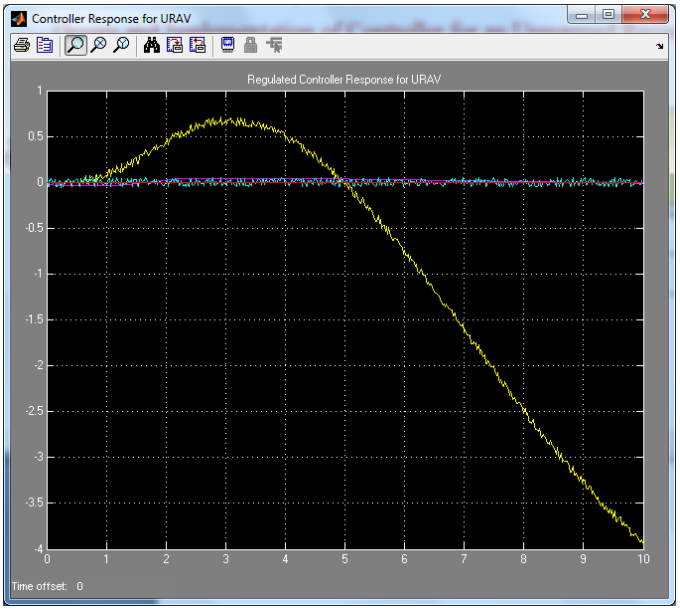

Fig.5. Regulated Controller Response for Global Hawk URAV

The controlled velocity response for Global Hawk URAV is illustrated in Fig.6. The red color response and yellow color response for velocity effects are steady state condition at 2000m/sec. The controlled thrust response for URAV is illustrated in Fig.7. The red color response for thrust effects are steady state condition at 2000m/sec.

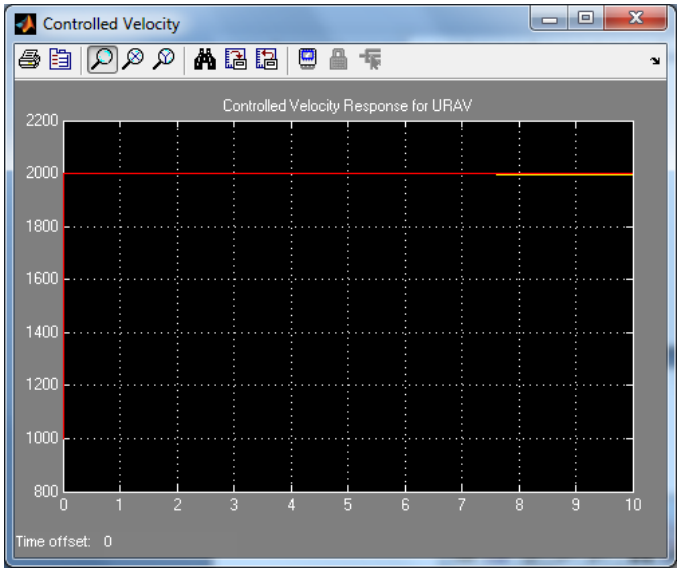

Fig.6. Controlled Velocity Response for URAV

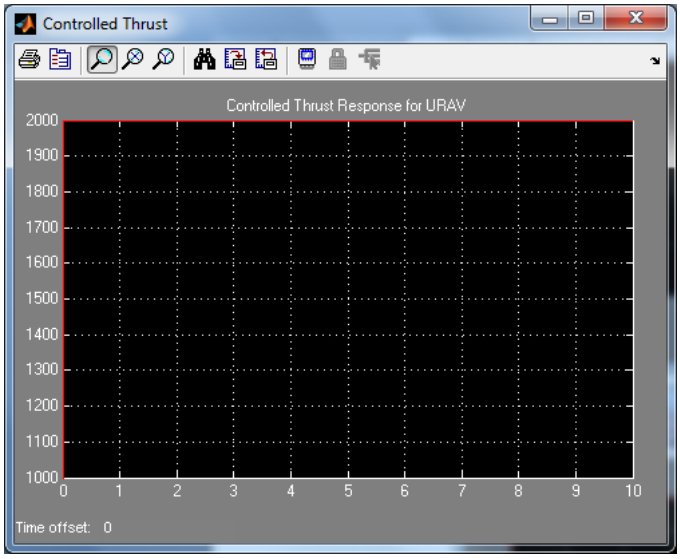

Fig.7. Controlled Thrust Response for URAV

VII. Conclusion

The SIMULINK model for observer controller design for Global Hawk URAV has two main response curves to analyze the stability. They are thrust and velocity effects of Global Hawk URAV with respect to time. According to this SIMULINK model, the stability analysis is developed by two effects such as velocity and thrust effects. The operation of observer controller is to express with elevator and thrust force analysis. The response for stability analysis for observer controller is also implemented by utilizing the appropriate MATLAB codes. The details description is also expressed in Appendix. The design process and tools investigated in this thesis allow the designer to obtain the regulated observer controller, model the closed-loop plant/controller system, and evaluate the controller's performance using MATLAB. In order to implement the controller with the given system, the observer controller is the best choice. The performance of this design was very similar to the performance

of the full state feedback controller. The velocity response has no overshoot. The pitch rate response was also very similar, except that it did not seem to settle out as quickly. Further analysis can be carried out to reduce the actuator saturation for the elevator rate by modifying the close loop feedback, K, in that system. Other than that actuator response, the observer controller design performed just as well as the full state feedback controller.

REFERENCES

[1] Ogata, Katsuhiko, Modern Control Engineering, 2002
[2] Dorf, Richard, and Bishop, Robert, Modern Control Systems, 2000
[3] Dixon, Warren, Control System Theory: EML5311, Course Notes, 2009
[4] ADMIRE aircraft model http://www.foi.se/admire (2005-12-20).
[5] The Mathworks Inc. http://www.mathworks.com (2005-12-20).
[6] J.W.C. Robinson, S.-L. Wirkander, M. Hammar and L. Forssell, Nonlinear Flight Control Design for a UAV, Swedish Defence Research
[7] Agency, FOI report, FOI-R–1863–SE, Oct. 2005.
[8] J.W.C. Robinson and M. H¨ogberg, Block Backstepping and Two-Timescale Control for Aircraft and Missiles, Swedish Defence Research Agency, FOI report, Manuscript in preparation.
[9] C. Schumacher and P.P. Khargonekar, "Stability Analysis of a Missile Control System with a Dynamic Inversion Controller," J. Guidance, Control and Dynamics, Vol. 21, No. 3, 1998, pp. 508–515.
[10] M. Athans and P. Falb, Optimal Control, McGraw-Hill, New York, NY, 1966.

AUTHORS

First Author – Chaw Ei San, Department of Electronic Engineering, Mandalay Technological University
Second Author – Hla Myo Tun, Department of Electronic Engineering, Mandalay Technological University
Third Author – Zaw Min Naing, Technological University (Maubin)